PROCEEDINGS of the
23rd International Congress on Acoustics
9 to 13 September 2019 in Aachen, Germany

Method of estimation of frequency spectrum and power of the sound generated by an unsteady flow through a sonic crystal

Viktor HRUŠKA(1), Michal BEDNAŘÍK(1), Milan ČERVENKA(1)

(1)Czech Technical University in Prague, Faculty of Electrical Engineering, Technická 2, 166 27 Prague 6, Czech Republic, viktor.hruska@fel.cvut.cz

Abstract

Although the importance of sonic crystals serving as sound barriers is growing, only a little interest was given to the sound emission from a sonic crystal due to windy weather conditions. The Curle's aeroacoustic analogy is reviewed in brief to obtain a suitable formulation for the low Mach number flow and rigid crystal structure. The radiation from the crystal has the dipolar characteristic and the dominating frequency corresponds to the Stouhal number 0.3. The values slightly exceeding 50 dB[A] were found for the radiation maxima at 20 m distance. It follows from the method design that it provides maximum estimate of the radiated power.

Keywords: sonic crystals, vortex sound, CFD simulations

INTRODUCTION

Special configurations of specifically shaped elements called sonic crystals are promising in the field of noise reduction. It can be shown that there are regions of frequency domain (band gaps) in which the crystal is effectively impermeable for sound waves (see e.g. [1] for further commentary). The major practical advantage of the sonic crystals is ease of their construction compared to noise barriers demanding solid foundations. Although there are various element shapes that can form a crystal lattice cell we limit ourselves to a simple yet common case of the crystal consisting of cylindrical rods.

In this work we investigate possible drawback of this approach. When the sonic crystal is situated outdoors the wind flowing past the rods might act as a source of sound. The topic is approached by numerical simulations of the turbulent flow with subsequent analysis by means of the vortex sound theory. The presented method calculates the maximum estimate of the radiated sound power.

THEORY

Sound generation from the airflow through a sonic crystal is inherently linked to the well-known phenomenon of flow instabilities past a cylinder. The Strouhal number St specific for the studied case is not predetermined, but we may assume it to lie between 0.2 – 0.4. Hence, we can assess that for rod diameters in centimeters and flow speeds around 10 m/s (fresh breeze) the flow instabilities frequency should be expected in tens of hertzs. The corresponding wavelength of the radiated sound is at least three meters, making not only the rods' diameter but also the height and the breadth of the crystal acoustically compact for many practical cases. It follows that the airflow through the crystal shall be regarded incompressible. For the same reasons we do not consider any interaction of the flow induced sound with the crystal stop-band. Usually they are at least one order of magnitude apart from each other for the outdoor situated noise barriers. To sum up these considerations, we can simulate the incompressible turbulent flow through the sonic crystal and then employ a suitable aeroacoustic analogy.

In his well-known pair of articles [2, 3] Lighthill proposed equivalency of the sound generated by the turbulence in the real fluid and the sound produced in the ideal and stationary medium with a source governed by the so called Lighthill stress. The resulting wave equation for density perturbations $\rho' = \rho - \rho_0$ propagating at the adiabatic sound speed c_0 in an unbounded Stokesian fluid reads [5]

$$\frac{\partial^2}{\partial t^2}\rho' - c_0^2\nabla^2\rho' = \nabla\cdot\left[\nabla\cdot\left(\rho\boldsymbol{uu} + \left(p' - c_0^2\rho'\right)\mathbb{I} - \boldsymbol{\sigma}\right)\right] \ , \tag{1}$$

where $\boldsymbol{u}$, p, $\mathbb{I}$ and $\boldsymbol{\sigma}$ denote the fluid velocity, pressure, the unit tensor and the viscous stress tensor respectively. The mean values are denoted with the subscript 0, the perturbation values with the prime $(\cdot)'$ (e.g. $p' = p - p_0$). In the limit of low Mach number Ma and high Reynolds number Re the pressure and density perturbations on the right hand side cancel each other, the viscous stresses are negligible compared to the Reynolds stresses $\rho_0\boldsymbol{uu}$. That leaves only the double divergence $\nabla\cdot[\nabla\cdot(\rho_0\boldsymbol{uu})]$ on the right hand side of Eq. (1).

In the presence of stationary solid body within the flow dipole sources emerge beside the free-field quadrupolar contributions. They are formally introduced by the so called Curle's aeroacoustic analogy resulting from the Lighthill's theory taking into account the source imaging due to the solid boundary presence. Let H denote the Heaviside step function defined as 0 for a point inside the body and 1 everywhere else. Let us suppose the low Mach and the high Reynolds number limit and the rigid body. The wave equation for the density perturbations then takes the form [5, 4]

$$\frac{\partial^2}{\partial t^2}\left(\mathrm{H}\rho'\right) - c_0^2\nabla^2\left(\mathrm{H}\rho'\right) = \nabla\cdot[\nabla\cdot(\mathrm{H}\rho_0\boldsymbol{uu})] - \nabla\cdot\left[\left(p'\mathbb{I} + \rho_0\boldsymbol{uu}\right)\cdot\nabla\mathrm{H}\right] \ . \tag{2}$$

The first source term corresponds to the previously investigated quadrupole source from the turbulent wake and its power is proportional to Ma^5. The second source term represents the reaction of the body surface to the unsteady flow. Its radiation characteristic is dipolar and its power proportional to Ma^3 for low Mach number [5]. Hence, the qudrupole contribution is negligible compared to the dipole one when $\mathrm{Ma}\to 0$. For a rigid body with the no slip velocity condition on its surface $\rho_0\boldsymbol{uu} = 0$ on the face of the body and therefore only the $p'\mathbb{I}$ term on the right hand side persists.

The following integral analogue of Eq. 2 is obtained by means of the three-dimensional free-space Green's function:

$$\left(\mathrm{H}c_0^2\rho'\right) = -\frac{\partial}{\partial x_i}\oint_S \frac{p'\left(t - \frac{|\boldsymbol{x}-\boldsymbol{y}|}{c_0}\right)}{4\pi|\boldsymbol{x}-\boldsymbol{y}|} n_i \ \mathrm{d}S(\boldsymbol{y}) \ , \tag{3}$$

where n_i is the ith component of the unit normal vector on the rod surface. In the far field (Fraunhofer) approximation ($|\mathbf{x}|\to\infty$, $p' = c_0^2\rho'$) it reads

$$p'(\boldsymbol{x},t) \approx \frac{x_i}{c_0|\boldsymbol{x}|^2}\frac{\partial}{\partial t}\oint_S p'\left(t - \frac{|\boldsymbol{x}|}{c_0} + \frac{\boldsymbol{x}\cdot\boldsymbol{y}}{c_0|\boldsymbol{x}|}\right) n_i \ \mathrm{d}S(\boldsymbol{y}) \ . \tag{4}$$

It follows that the far field acoustic pressure can be calculated from the known unsteady pressure on the rods' faces obtained by a suitable numerical simulation. Since the rods' diameter is small compared to the typical wavelengths we disregard any diffraction effects. The integral in Eq. (4) represents the force exerted on the surface of the rod by the fluid. For an isolated cylinder the net force is usually predominantly perpendicular to the free flow direction and therefore it is sometimes called lift (force). Because the relation of the complicated flow inside the crystal to the free flow is nontrivial we don't use this designation. However, as it will be shown below, the radiated sound directivity suggests that the overall effect of the unsteady forces is "rather a lift than a drag".

NUMERICAL EXPERIMENTS

The numerical results presented below was simulated using Comsol Multiphysics software, version 5.4. The fluid dynamics simulations employed the Single-phase Turbulent flow interface with the Shear Stress Transport

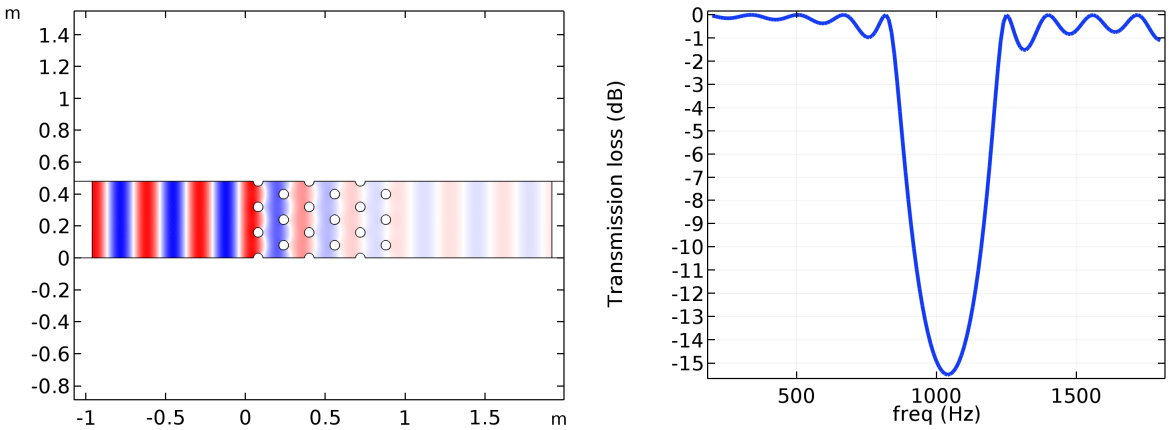

Figure 1. Example of a monofrequency plane wave (1040 Hz) propagating through the studied sonic crystal (left), transmission loss of the crystal (right) in the direction depicted left.

model (i.e. the Unsteady Reynolds Averaged Navier Stokes Equations – URANS – approach, see e.g. [6]). The inflow velocity was 12 m/s (corresponding to a fresh breeze), the open boundary condition is imposed on all other boundaries. The auxilliary acoustic simulations were made within the Pressure acoustics environment. Subsequent treatment of the simulated data was made using our own code in GNU Octave environment.

3.1 The studied case

In order to bring the simulations close to a real example we first review the features the sonic crystal exhibits as a sound barrier. Assuming that the outdoor placed crystals shall prevent primarily the traffic noise it is reasonable to tune the configuration to have a band-stop around 1 kHz. In the following a hexagonal lattice with the lattice constant 0.13 m and the rods' diameter 60 mm is studied. The transmission loss (assuming invsicid and thermally nonconducting air without mean flow) and an example of wave propagating through the crystal are in Fig. 1.

3.2 Restriction to two dimensions

Although the turbulence is essentially a three dimensional phenomenon, we might make use of the fact that the variation of pressures and velocities is much more pronounced across the rods then along them. A simplified example is depicted in Fig. 2 (the symmetry boundary condition is imposed on the top and the bottom of the domain). The isosurfaces of unsteady pressure are virtually invariant along the z direction. Naturally, we cannot fully exclude the surface pressure perturbations along the height of the rods, especially further inside the crystal, we just assume them to be significantly weaker than the azimuthal perturbations.

On the other hand, a complete restriction to the planar description (e.g. using the 2D instead of the 3D Green's function in Eq. (4)) would lead to a considerable overestimation of the radiated sound power. Therefore, we suggest to extrude the planar flow solution to three dimensions and employ Eq. (4) on the rods's surfaces disregarding the bases.

Weak phase differences along the height of the rod (which would not be captured by the suggested approach) are possible. Nevertheless, their near field effects would lead to weaker far field radiation and so we are getting the maximal radiated power estimation.

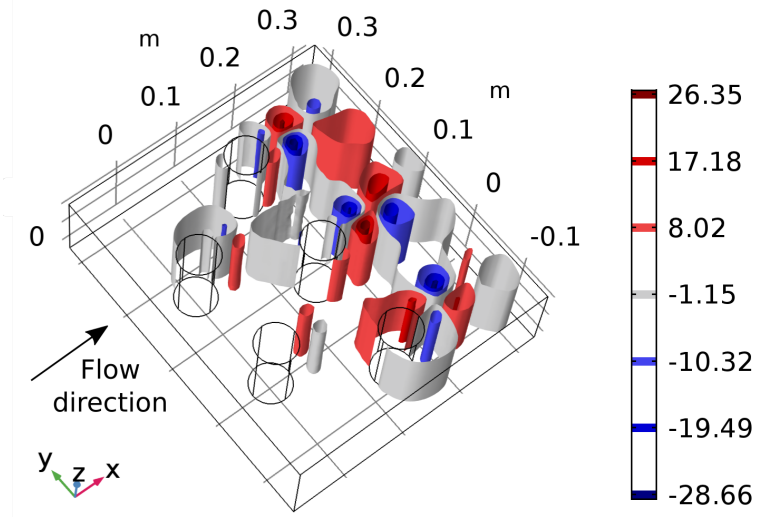

Figure 2. Instantaneous isosurfaces of pressure petrurbations $p' = p - p_0$, where $p_0(\boldsymbol{x}) = 1/T \int_0^T p(\boldsymbol{x})\mathrm{d}t$ with T being a period of steady oscillations. The colorbar values are in pascals.

3.3 Sound power and spectrum based on extrusion

A planar set-up consisting of 18 rods in 6 columns was simulated. A snapshot of the instantaneous velocity field is depicted in Fig. 3. The von Kármán vortex street is not formed inside the crystal. However, the trailing wakes behind the cylinders are unstable and therefore pressure perturbations of the cylinders' faces occur.

Eq. (4) is employed in a discretized form. The radiated pressure is evaluated on a circle with the center in the midpoint of the crystal and of the 20 m radius. The radiated sound spectrum is dominated by the frequency 62.5 Hz (see Fig. 4), corresponding to the Strouhal number of 0.31 (the rods' diameter is the characteristic length).

In Fig. (4) the sound pressure level (in dB[A]) of the dominant frequency is depicted as the height and the color is governed by the phase angle. It is evident that the sound radiation from the crystal resembles a dipole with nulls at the inflow direction.

DISCUSSION

Limitations of the presented method depends on the validity of various assumptions. First, the URANS approach neglects some of the turbulent nonlinearities propagating through the crystal. The main mechanism is captured correctly but some subtleties regarding the perturbations along the rods' height and fine tuning of the flow synchronization might have been left out. A logical step in the future research is therefore a comparison between the URANS and the Large Eddy Simulation (LES) in a benchmark case. Second, the imperfections of the extrusion technique should be better quantified and further tested. Another point of high interest is the stability of Strouhal number with varying inflow speed and crystal geometry.

The Curle's formulation under conditions allowing for the volume sources to be neglected is well-suited for the Boundary Element Method (BEM), which might be employed instead of the Green's functions.

The calculations disregards the reflections from the ground. Although many of the surface types (e.g. grass) have low reflection coefficient for almost grazing incidence, which would be the case, this topic should be closely discussed in the future.

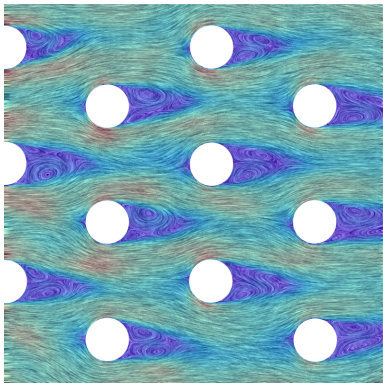

Figure 3. Instantaneous velocity field around the crystal center visualized by the Line Integral Convolution.

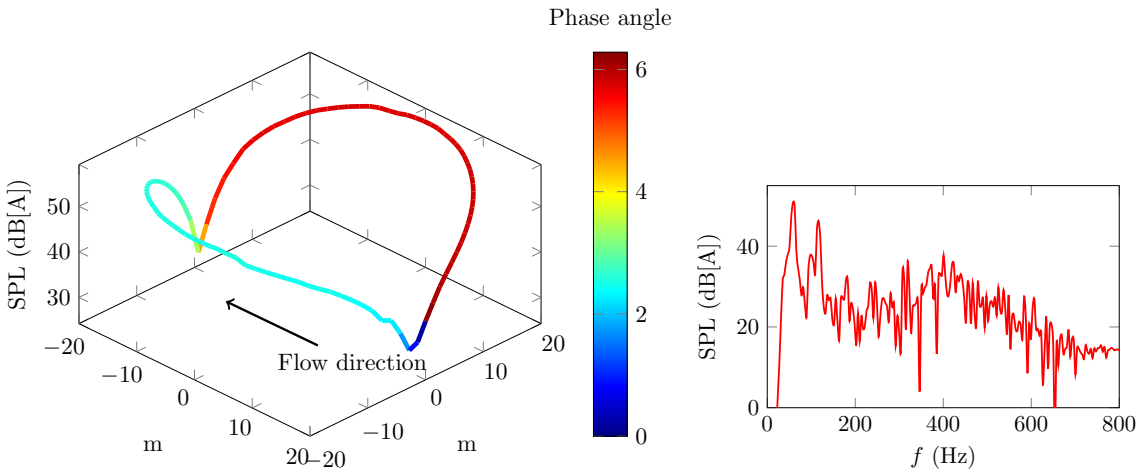

Figure 4. Left: Sound pressure level (SPL) and phase angle of the dominant frequency evaluated on the circle of 20 m radius surrounding the sonic crystal. Right: Spectrum of the emmited sound in the main radiation direction.

Note that for the noise hygiene purposes the effect of low frequency on the human perception has to be counted in (e.g. by conversion of decibels to phones). Generally, the low frequency noise is not percieved as loud as the benchmarks around 1 kHz (cf. e.g. [7]).

CONCLUSIONS

The method of estimating the radiated spectrum and sound power generated from the flow through a sonic crystal was designed, tested and discussed. The sonic crystal under windy weather conditions radiates the sound with the dipolar characteristic and the fundamental frequency corresponding to the Strouhal number 0.3. Since some of the loss mechanisms were disregarded the method provides the maximum estimate of the radiated power (ca. 55 dB[A] in the main radiation direction).

The future goals include benchmarking of the method with the LES, study of the Strouhal number stability and comparison of the results obtained employing the Green's functions with the BEM simulations.

ACKNOWLEDGEMENTS

This work was supported by the GACR grant No. 18-24954S and by the Grant Agency of the Czech Technical University in Prague, grant No. SGS19/107/OHK3/2T/13.

REFERENCES

[1] Ming-Hui Lu, Liang Feng, and Yan-Feng Chen. Phononic crystals and acoustic metamaterials. *Materials Today*, 12(12):34–42, dec 2009.

[2] M. J. Lighthill. On sound generated aerodynamically. i. general theory. *Proceedings of the Royal Society of London. Series A, Mathematical and Physical Sciences*, 211(1107):564–587, 1952.

[3] M. J. Lighthill. On sound generated aerodynamically. ii. turbulence as source of sound. *Proceedings of the Royal Society of London. Series A, Mathematical and Physical Sciences*, 222(1148):1–32, 1954.

[4] N. Curle. The influence of solid boundaries upon aerodynamic sound. *Proceedings of the Royal Society A: Mathematical, Physical and Engineering Sciences*, 231(1187):505–514, sep 1955.

[5] M. S. Howe. *Theory of Vortex Sound*. Cambridge University Press, Cambridge, 2002.

[6] Mehrzad Tabatabaian. *CFD module*. Mercury Learning and Information,, Dulles, Virginia :, 2015. Mehrzad Tabatabaian., Includes bibliographical references (pages 191-197) and index.

[7] William M. Hartmann. *Signals, Sound, and Sensation (Modern Acoustics and Signal Processing)*. American Institute of Physics, 2004.